Theor Chim Acta (1994) 88: 299–310

Theoretica Chimica Acta

On the origin of the barriers and the structures of acetaldehyde in its ground and first singlet excited state

C. Muñoz-Caro[1], A. Niño[1], D. C. Moule[2]

[1] Departamento de Informática, Universidad de Castilla-La Mancha, Ronda de Calatrava s/n, 13071 Ciudad Real, Spain

[2] Department of Chemistry, Brock University, St. Catharines, Ont., L2S3A1, Canada

Received February 5, 1993/Accepted September 14, 1993

Summary. An *ab initio* study of the ground and the first singlet excited states of acetaldehyde has been performed to analyze the molecular properties as a function of the methyl torsion and the aldehydic hydrogen wagging angles. The structural characteristics and the conformational behaviour in both electronic states have been determined. The important structural changes between the two states have been analyzed by a decomposition of the total energy into its components. It was found that the methyl torsion barriers arise mainly from attractive interactions. Evidence is presented which shows that these barriers arise from in-plane and out-of-plane hyperconjugative effects involving the oxygen atom. It is also shown that the pyramidalization experienced by the carbonyl carbon in the first singlet excited state has two sources, namely, a decrease in the electronic repulsion and an increase in the electron–nucleus attraction.

Key words: Hyperconjugation – Origin of barriers – Acetaldehyde – Internal rotation – Wagging

1 Introduction

Acetaldehyde, CH_3CHO, is the molecular prototype for the aliphatic carbonyl series of compounds from the standpoint of the photochemical and spectroscopic properties. Its structural characteristics and spectra have been reviewed recently by Clouthier and Moule [1] and have been related to similar molecules with progressively heavier atoms. The transition between the ground and first singlet excited state is of the $n \rightarrow \pi^*$ type and is localized in the carbonyl group. The vibronic spectrum which lies in the near UV is complicated and congested as a result of the interaction of the internal methyl rotation and the out-of-plane aldehydic hydrogen wagging motions [2].

Correspondence to: C. Muñoz-Caro

Several theoretical *ab initio* studies on the molecular structure and methyl torsion barrier of acetaldehyde have been reported for the ground state. The first partial geometry optimization was carried out by Del Bene et al., using a minimal basis set with C_3 symmetry for the methyl group [3]. Later, Bernardi et al. performed full geometry optimization with the same basis set, for planar and staggered conformations [4]. Full geometry optimization using split-valence (4-31G) and polarized (6-31G*) basis set with Møller–Plesset corrections for correlation energy were performed by Wiberg et al. for selected conformations [5, 6]. The most recent calculation is that of Ozkabak and Goodman who used a 6-31G** basis set with and without Møller–Plesset correction. These authors carried out a conformational study on the methyl torsion angle, with full geometry optimization [7].

The structural calculations for the S_1 first $n\pi^*$ excited state are not as complete as those of the S_0 ground state. Crighton and Bell performed partial geometry optimization for selected conformations with Dunning–Huzinaga type basis sets. They determined the torsion-inversion barriers with a model which used C_3 symmetry for the methyl group [8]. Baba et al., using a similar basis set with addition of polarization functions and C_3 methyl symmetry, performed a partial conformational analysis of the S_0 and S_1 states without optimization [9].

All of these theoretical studies show that in the S_0 ground state the molecule is planar with a methyl hydrogen eclipsing the oxygen atom. These results are confirmed by microwave studies [10]. In contrast, the most stable structure for the S_1 excited state has an antieclipsed (staggered) conformation when the CCO frame is fixed into a plane. As in the case of formaldehyde, the aldehydic hydrogen distorts from the plane of the frame. Thus, both the methyl torsion and aldehydic wagging coordinates are displaced on excitation to the S_1 excited state [2, 11].

The origin of the torsional barrier in the S_0 state has been a matter of controversy since the late sixties [12]. A covalent-like in-plane methyl hydrogen–oxygen interaction [13] or an hyperconjugative effect [9, 14, 15] have been suggested to be important in determining the barrier to internal rotation. On the other hand, apart from a simple application of Walsh rules [16], no detailed explanation has been given for the origin of the inversion barrier.

In this paper we present a comparative theoretical study of the S_0 and S_1 electronic states of acetaldehyde. A complete conformational analysis of the methyl torsion and aldehydic hydrogen wagging coordinates has been performed. Complete molecular geometry optimization at each point has been carried out without the C_3 symmetry constraint on the methyl group. Our aim is to analyze the structural features of acetaldehyde in the two electronic states, to discuss the differences in their molecular properties and to gain a deeper insight into the origin of the torsional and inversion barriers.

2 Methods

In this work, all calculations have been carried out by *ab initio* methodology through the use of the GAMESS package [17]. The basis set used has been a 4-31G** constructed from the 4-31G* with addition of p orbitals on the hydrogen (exponent of 1.1, the value used in the standard 6-31G** set [18]). The RHF approximation has been used in the treatment of the ground state, S_0 and ROHF approximation for the first singlet excited state, S_1. Electronic correlation has not been used because it has been shown to have a small effect on the torsional

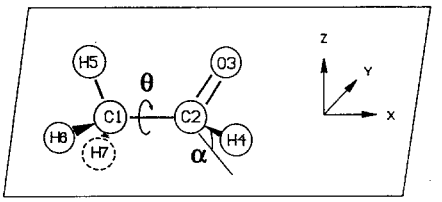

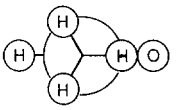

ECLIPSED

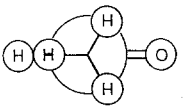

ANTIECLIPSED

Fig. 1. The numbering convention and the Newman projections for the eclipsed ($\theta = 0°$) and the antieclipsed ($\theta = 60°$) conformations in planar ($\alpha = 0°$) acetaldehyde.

barrier of acetaldehyde [6, 7]. On the other hand, the HF approximation without correlation reproduces the inversion in molecules [8, 19]. Thus, it is possible to use HF wavefunctions for discussing the origin of the inversion barriers at least in a qualitative fashion. Potential surfaces were obtained for a grid size of 60° and 10° for the methyl torsion and aldehydic wagging angles respectively. The methyl torsion angle is defined as dihedral angle $\theta(H_5{-}C_2{-}C_1{-}O_3)$, whereas the wagging angle, α, is expressed by means of the out-of-plane angle from bond $H_4{-}C_1$ to plane $C_2{-}C_1{-}O_3$. The angles are defined with respect to the numbering system shown in Fig. 1. As a reference for the planar conformations, we will always assume H_5 to lie in plane and H_6, H_7 to be out of plane.

Geometry optimization was carried out by means of the Broyden–Fletcher–Goldfard–Shanno algorithm [20]. The starting geometry for every molecular optimization was taken from microwave data [10, 21]. The optimization procedure was carried out until the largest component of the gradient was less than 5×10^{-4} hartree/bohr or hartree/rad and the root mean square gradient less than 1.7×10^{-4} hartree/bohr or hartree/rad.

3 Results and discussion

A Structural and conformational results

Table 1 compares the experimental microwave geometry with the optimized geometry for the most stable configuration. As would be expected, the CCHO frame of the molecule is planar with a hydrogen atom from the methyl group eclipsing the oxygen atom. The results also show that the bonds of the methyl group are not equivalent, with the out-of-plane CH bonds being 0.005 Å longer than the CH in-plane bond. McKean has shown from a correlation of the isolated CH stretching frequencies that the CH out-of-plane bond in acetaldehyde is 0.006 Å longer than in the in-plane bond [22]. The CCH_{ip} and CCH_{oop} angles also reflect these differences. The calculated bond lengths are found to agree well with the experimental values, although almost all are slightly too short. This trend may be attributed to the neglect of electron correlation. The calculated bond angles show a reasonable correspondence with the experimental data giving typical values for sp^2 and sp^3 hybridization for the C_2 and C_1 atoms respectively.

Table 1. Experimental and optimized structural parameters for the S_0 and the S_1 electronic states of acetaldehyde

Parameters[a]	Microwave geometry[b]	S_0 eclipsed	S_1	
			Antieclipsed	Pyramidal frame
C_1–C_2	1.501	1.502	1.488	1.498
C_2–O_3	1.204	1.185	1.362	1.362
C_2–H_4	1.124	1.097	1.069	1.080
C_1–H_5	1.079	1.081	1.083	1.083
C_1–H_6	1.102	1.086	1.087	1.088
C_1–H_7	1.102	1.086	1.087	1.084
C_1–C_2–O_3	124.7	124.38	117.27	113.99
H_4–C_2–C_1	113.9	115.18	127.41	119.40
H_5–C_1–C_2	110.7	110.23	109.71	109.95
H_6–C_1–C_2	109.2	109.76	111.58	111.20
H_7–C_1–C_2	109.2	109.76	111.58	110.72
H_6–C_1–C_2–H_5	—	−121.20	−119.84	−120.21
H_7–C_1–C_2–H_5	—	121.20	119.84	119.73
Torsion angle	—	0.00	60.00	57.37
Wagging angle	—	0.00	0.00	37.83

[a] In angstroms and degrees.
[b] From Ref. [21].

The equilibrium structure for the S_1 state was calculated to be very different from the S_0 ground state in several important ways. The Walsh correlation diagram [16] predicts that the aldehyde frame of the molecule should be nonplanar in the $n\pi^*$ excited state as a result of the population of the π^* orbital. Our calculations show the CH aldehyde bond to be directed out of plane from the CCO group by 37.83°. This distortion in the frame also leads to displacements of the torsional angle. We found that $\theta = 57.37°$ for the equilibrium position. However, as shown in Table 1, the most striking feature is the change in the C_2–O_3 bond length from 1.185 Å of the S_0 state to 1.362 Å, which agrees with the standard values for double (1.16–1.22 Å) and single (1.36 Å) C–O bond lengths [23]. Bonding changes are analyzed using the overlap population (the magnitude is related to the intuitive idea of bond order). We observe that the C_2=O_3 bond order decreases greatly when going from the S_0 to the S_1 state (S_0/S_1: 1.147/0.351). Thus, the lengthening of the C_2=O_3 bond is associated with a loss of bonding interaction.

The potential energy surfaces obtained for the S_0 and S_1 electronic states with full geometry optimization are shown in Figs. 2 and 3. In agreement with previous work, a planar oxygen eclipsed conformation is found as the most stable form for the ground state, whereas an oxygen antieclipsed conformation is the most stable conformer for the first excited electronic state in the planar case. The minimum in the S_1 state is found to be the pyramidal conformation ($\theta = 57.37°$, $\alpha = 37.83°$). The calculated barrier to methyl rotation for the S_0 state is 378.8 cm^{-1}, in good agreement with the most recent experimental result, 407.7 cm^{-1} [24].

In the S_1 state, the obtained methyl torsion barrier of 677.9 cm^{-1} for the equilibrium case reproduces the experimental result, 687.0–691.0 cm^{-1} [11] within the error limits. On the other hand, our inversion barrier of 1093.0 cm^{-1} is almost

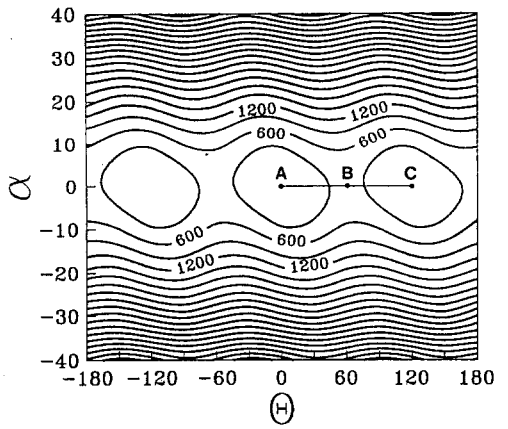

Fig. 2. The potential energy surface for acetaldehyde in the ground state. The interval between the isopotential lines is 300 cm^{-1}.

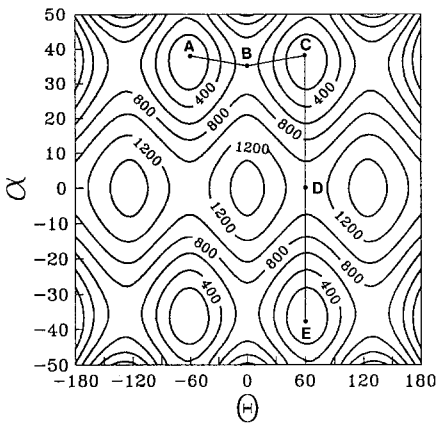

Fig. 3. The potential energy surface for acetaldehyde in the first singlet excited state. The interval between the isopotential lines is 200 cm^{-1}.

twice the observed value of 541.0–670.0 cm^{-1} [11], but it is similar to the 1371 cm^{-1} value given by Crighton and Bell [8].

Figures 2 and 3 permit us to analyze the dynamical behaviour of the system. In the S_0 state, Fig. 2, rotation of the methyl group from the eclipsed A (0°) to the eclipsed C (120°) conformation traverses the saddle point B (60°). The motion surmounts the torsion barrier without variation of the wagging angle. The wagging potential shows the quadratic shape of a harmonic oscillator.

In the S_1 state, Fig. 3, the methyl rotation between minima A ($\theta = -60°$, $\alpha = 37.83°$) and C ($\theta = 60°$, $\alpha = 37.83°$) traverses a rotation barrier through saddle point B ($\theta = 0°$, $\alpha = 35°$) with a small variation of the wagging angle. On the other hand, from equilibrium position C, the wagging angle moves onto equilibrium configuration E ($\theta = 60°$, $\alpha \cong -37.83°$) traversing the inversion barrier through saddle point D ($\theta = 60°$, $\alpha = 0°$). In this case, the torsion angle experiences little variation. Thus, in the S_1 state, torsion and wagging become large amplitude movements and they cannot be described by a harmonic model.

Table 2. Energy components[a] for some selected conformations in the S_0 and S_1 states of acetaldehyde

	S_0		S_1		
	Eclipsed	Antieclipsed	Eclipsed	Antieclipsed	Pyramidal frame
T	151.76369	151.76392	151.68028	151.68691	151.70175
V_{en}	−498.74518	−498.71773	−492.37823	−492.62545	−492.96481
V_{ee}	123.80803	123.80370	120.79232	120.90624	121.04574
V_{nn}	70.39779	70.37616	67.23267	67.35752	67.53755

[a] In atomic units, all coordinates were fully optimized

B Origin of the methyl torsion barriers

To investigate the interaction responsible for the torsion barrier in the S_0 state, we analyze the components which contribute to the total energy. Table 2 collects the kinetic T, and potential, V_{en}, V_{ee}, V_{nn} energy terms for the planar conformations in the S_0 state. These components are assumed to be reliable, since the virial theorem is satisfied (the molecular optimization procedure yields very small values of the root mean square gradient: 0.00008 hartree/bohr or hartree/rad in the worst case). The factor determining the barrier in the S_0 electronic state is the change in the electron–nucleus interaction, $\Delta V_{en} > \Delta T + \Delta V_{ee} + \Delta V_{nn}$. The highest absolute value of V_{en} is found for the most stable conformation, −498.74518 a.u. Thus, the barrier results from a decrease in the attractive interaction term, V_{en}. This fact is in total agreement with previous results for the S_0 state obtained with fixed geometry and where the virial theorem was satisfied by scaling [13, 14, 25].

In order to elucidate the individual interactions which are responsible for the barrier, we decompose the V_{en} term into its atomic components. We use the relationship

$$\sum_{\alpha}^{N} Z_\alpha V_\alpha^{elec} = 2V_{nn} + V_{en}, \tag{1}$$

which relates the electrostatic potential, V_α^{elec}, on the α atom with nuclear charge Z_α, to the global potential energies V_{nn} and V_{en} [26]. Taking into account that, in atomic units,

$$V_{nn} = 1/2 \sum_{\alpha}^{N} \sum_{\beta \neq \alpha}^{N} \frac{Z_\alpha Z_\beta}{R_{\alpha\beta}}, \qquad V_{en} = -\sum_{\alpha}^{N} \sum_{i}^{n} \left\langle \phi_i \left| \frac{Z_\alpha}{r_{i\alpha}} \right| \phi_i \right\rangle, \tag{2}$$

with n equal to the number of electron and ϕ_i the one-electron wavefunction, the substitution of (2) into (1) yields, after rearrangement

$$-\sum_{\alpha}^{N} \left[\sum_{i}^{n} \left\langle \phi_i \left| \frac{Z_\alpha}{r_{i\alpha}} \right| \phi_i \right\rangle \right] = \sum_{\alpha}^{N} \left[Z_\alpha V_\alpha^{elec} - \sum_{\beta \neq \alpha}^{N} \frac{Z_\alpha Z_\beta}{R_{\alpha\beta}} \right]. \tag{3}$$

This permits us to define an average electron attraction on a nucleus α as

$$V_{en}(\alpha) = Z_\alpha V_\alpha^{elec} - \sum_{\beta \neq \alpha}^{N} \frac{Z_\alpha Z_\beta}{R_{\alpha\beta}}. \tag{4}$$

The electrostatic potential, V_α^{elec} is obtained by the GAMESS package and the nuclear repulsion is calculated from the molecular structure. The $V_{en}(\alpha)$ terms

Table 3. Electron–nucleus attraction on each nucleus[a] for the planar conformations of acetaldehyde in the S_0 and the S_1 states

	S_0		S_1	
	Eclipsed	Antieclipsed	Eclipsed	Antieclipsed
C_1	−121.58189	−121.55852	−121.29824	−121.39492
C_2	−128.95278	−128.88159	−126.62495	−126.69652
O_3	−216.71849	−216.78646	−213.11928	−213.19334
H_4	−8.15527	−8.13949	−8.04493	−8.04810
H_5	−7.96128	−7.62604	−7.99802	−7.62498
H_6	−7.68773	−7.86280	−7.64638	−7.83400
H_7	−7.68773	−7.86280	−7.64638	−7.83400
H_{methyl}	−23.33674	−23.35164	−23.29078	−23.29298

[a] In atomic units

obtained from Eq. (4) are shown in Table 3. This table may be used to give a detailed insight into the source of the barrier. For example, in the eclipsed conformation the in-plane hydrogen always provides the greatest stabilization. For the S_0 ground state: H_5/H_6 −7.96128/−7.68773 a.u. In the antieclipsed conformation the situation is reversed: −7.62604/−7.86280 a.u. In this table, the contributions of the three hydrogens of the methyl group are shown as H_{methyl}. Thus, the contribution of the methyl hydrogens favour the antieclipsed conformation. It follows therefore that the conformational preference is determined by the stabilization of the atoms which constitute the frame. That is, it appears as if the methyl hydrogens have the effect of perturbing the adjacent atoms of the group and altering their energies. At the same time, they themselves do not appear to be greatly affected. It is the contribution of C_1, C_2 and H_4 atoms which stabilizes the eclipsed conformation in the S_0 ground state. It follows that the barrier must arise from global effects, involving all parts of the molecule and not just the methyl moiety. This fact is in agreement with the Ozkabak and Goodman conclusion that skeletal flexing is one important determinant of the methyl torsion potential shape in acetaldehyde [7].

An analysis of the electronic distribution can be made through the use of electron density maps. To clarify the differences between the eclipsed and antieclipsed conformations electron density difference maps were constructed. Figures 4a and 4b have been obtained as $\Delta\rho = \rho(\text{eclipsed}) - \rho(\text{antieclipsed})$. In the S_0 state, it is clear in Fig. 4a that a higher electron density appears in the internuclear C_1–C_2 zone. On the grounds of the Hellmann–Feynman theorem [27] this can be interpreted as a higher bond character in the C_1–C_2 bond for the eclipsed conformation. This agrees with the changes in the C_1–C_2 bond length from an eclipsed to an antieclipsed value of 1.502/1.509 Å and an overlap population of 0.685/0.675. This fact also agrees with the previous results that show a change in the π C_1–C_2 bond density component for the eclipsed conformation [9]. This change in electron density is one factor that contributes to the stability of the electron–nucleus interaction which is given in Table 3 for the C_1 and C_2 atoms in the eclipsed conformation. It is not yet clear, however, how this variation in electron density is produced.

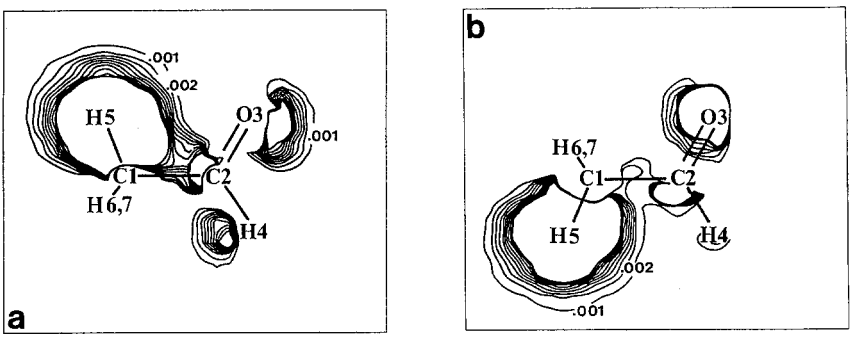

Fig. 4a, b. Electronic density difference maps in acetaldehyde for the planar conformations. The interval between lines is 0.001 e/Bohr^3. **a** Excess of density in the eclipsed conformation of the S_0 ground state (ρ(eclipsed) − ρ(antieclipsed)). **b** Excess of density in the antieclipsed conformation of the S_1 excited state (ρ(eclipsed) − ρ(antieclipsed)).

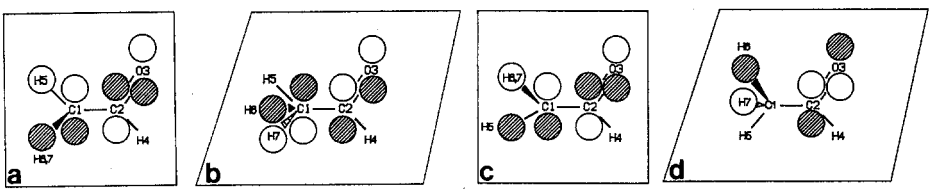

Fig. 5a–d. Molecular orbitals showing the π_y and the π_z methyl pseudoatom contributions for acetaldehyde. The dotted circles show the negative lobes. **a** π_y contribution in the eclipsed conformation of the ground state. **b** π_z contribution in the eclipsed conformation of the ground state. **c** π_y contribution in the antieclipsed conformation of the excited state. **d** π_z contribution in the antieclipsed conformation of the excited state.

In the S_0 state hyperconjugation has been invoked as a single source of the methyl rotation barrier in acetaldehyde. The usual treatment of hyperconjugation is to assume that the three methyl hydrogens act as a single pseudoatom [28]. The orbitals corresponding to that entity are obtained by a linear combination of the 1s orbitals on the hydrogens. Using our axis nomenclature, the two π orbitals found in such a way are: $\pi_y = 1/\sqrt{6}(s(H_6) + s(H_7) - 2s(H_5))$, $\pi_z = 1/\sqrt{2}(s(H_6) - s(H_7))$, where the π_y is an in-plane orbital and the π_z is an out-of-plane orbital. Hyperconjugation is assumed to act as an out-of-plane effect. In addition, McKean has shown that the hyperconjugation produces a difference about 28–41 cm^{-1} between the in-plane and out-of-plane stretching frequencies of methyl CH bonds [22]. The experimental frequency difference [22] in acetaldehyde is 57 cm^{-1} which seems to be too high to be attributed purely to the usual hyperconjugative effect.

The problem was analyzed from the molecular wavefunctions taking into account the in-plane π_y orbital of the methyl hydrogen pseudoatom as well as the out-of-plane π_z orbital. Figure 5a shows the in-plane molecular orbital with the π_y contribution. The sign of the individual participations was found to be $+\pi_y + C_1 - C_2 + O_3$. Thus, we can postulate the existence of an in-plane bonding interaction between the positive lobe of the π_y orbital and the closer $2p_y$ orbital

of the O_3 atom. In the antieclipsed conformation the positive lobe of the π_y orbital is associated with the $H_{6,7}$ atoms and is more diffuse. Thus, the bonding interaction between the π_y and the $2p_y$ atomic orbitals of the O_3 atom is weakened as θ rotates from the eclipsed to the antieclipsed form. On the other hand, our molecular wavefunction shows two p_z type molecular orbitals. The first, with contributions $+\pi_z + C_1 + C_2 + O_3$ is very low in energy. The second p_z molecular orbital is much closer in energy to the HOMO orbital. Figure 5b shows its individual contributions: $-\pi_z - C_1 + C_2 + O_3$. In the antieclipsed conformation, the antibonding contribution increases when the π_z orbital approaches the $2p_z$ orbital of the O_3 atom. Therefore, in-plane and out-of-plane effects both contribute to the stabilization of the eclipsed conformation. We can attribute this antibonding interaction to the decrease of charge on the $H_{6,7}$ atoms, 0.864 to 0.845, as the molecule rotates to the antieclipsed form. Assuming that this charge goes to the $2p_z$ orbital of the C_1 atom, the shortening in the $H_{6,7}$–C_1 bond length, 1.086/1.084 Å, can be explained by an enhancement in the bonding interaction between the π_z and the $2p_z$ orbitals. At the same time, the $2p_z$ population on the C_1 atom changes from 1.064 to 1.100 and produces an increase in the antibonding C_1–C_2 interaction for the antieclipsed case. Thus it is possible to explain the lengthening of the C_1–C_2 bond length by the change in electron density in the C_1–C_2 internuclear zone.

Hyperconjugation has also been used to describe the methyl torsion barrier in the S_1 electronic state. It is not clear, however, how the same effect can reverse the S_0 methyl conformation. We begin by analyzing the components of the total energy. Table 2 shows that the principal factor responsible for the torsion barrier is the electron–nucleus interaction, $\Delta V_{en} > \Delta T + \Delta V_{ee} + \Delta V_{nn}$. In this case, the highest negative value of V_{en} is found for the antieclipsed conformation, -492.62545 a.u. Thus, the methyl torsion barrier in the upper electronic state is also the result of attractive interaction terms and is not due to steric hindrance which would be reflected as a repulsion $\Delta V_{en} < \Delta T + \Delta V_{ee} + \Delta V_{nn}$. The V_{en} total interaction term was decomposed by the technique previously given. The results given in Table 3 for the eclipsed and the antieclipsed cases show that all of the atoms contribute favourably to the antieclipsed conformation. It may be noted also, that H_{methyl} displays a similar behaviour to the S_0 state.

As was done for the S_0 state, a comparison between the electronic density distribution in the eclipsed and antieclipsed conformations should be useful in describing the specific interactions that lead to the conformational preference in the S_1 excited state. Figure 4b shows the excess electron density in the antieclipsed conformation with respect to the eclipsed case. In this map we observe a zone of electron density between the C_1 and the C_2 atoms. This behaviour in the S_1 antieclipsed conformation is similar to that of the S_0 eclipsed case (Fig. 4a). This fact explains the opposite contributions of the C_1 and C_2 atoms to the total electron–nucleus interaction in each electronic state (Table 3). The behaviour of the π_y and π_z orbitals of the pseudoatom was analyzed through the use of the molecular wavefunction. The π_y orbital was found in only one of the molecular orbitals and is shown in Fig. 5c. On the other hand, the highest energy out-of-plane molecular orbital was found to be a HOMO and is shown in Fig. 5d. The sign of the $2p_y$ contributions was $+\pi_y + C_1 - C_2 + O_3$, as in the S_0 state and the $2p_z$ contributions were $-\pi_z + C_2 - O_3$. Thus, the π_y orbital favours the eclipsed conformation. On the other hand, the π_z contribution prefers the antieclipsed form where the bonding interaction between the π_z and the $2p_z$ orbital of the O_3 atom is maximized.

The analysis of the change in the electronic population can provide further insight. Mulliken electronic population shows that on excitation from the S_0 to the S_1 state, the electronic charge on the C_2 atom increases from 5.622 to 5.865 and decreases on the O_3 atom from 8.480 to 8.326. Similar results are obtained for each conformations. These effects may be attributed to the redistribution of electronic charge on the C_2=O_3 moiety and to a charge localization in the neighbourhood of the C_2 atom. We can analyze the C_2=O_3 group through the $2p_z$ gross electronic populations. On excitation, the values for the eclipsed conformations change from 0.655 to 1.050 for the C_2 atom and from 1.332 to 1.923 for the O_3 atom. Also, the population on the $2p_y$ orbital of the O_3 atom decreases on excitation from 1.538 to 1.323 in the eclipsed conformation. Similar results are found for the antieclipsed conformation. Thus, in the S_1 state, the C_2 atom retains an electron in the $2p_z$ orbital and as a result the electronic density diminishes around the oxygen. This results in a rearrangement of the electronic structure around the oxygen atom and produces a shared pair of electrons on the $2p_z$ oxygen orbital and an electron in the $2p_y$ orbital. This picture is in agreement with the usual interpretation of an $n \rightarrow \pi^*$ transition where an electron is lifted from the nonbonding n orbital and placed in the antibonding π^* orbital of the C=O group. It is possible to attribute the decrease of charge in the $2p_y$ orbital of the O_3 atom to a weakening in the bonding interaction with the π_y pseudoatom orbital. However, the increase of charge in the $2p_z$ orbital of the O_3 atom reinforces its bonding interaction with the π_z orbital in the antieclipsed conformation. The result is the change from eclipsed to antieclipsed conformation when the excitation occurs. The bonding interaction between the π_z orbital and the $2p_z$ orbital on the O_3 atom could explain the decrease of the C_1–C_2 bond length from 1.491 to 1.487 Å and the increase of the electronic density in this internuclear zone as the molecule rotates from the eclipsed to the antieclipsed form.

C Origin of the inversion barrier in the S_1 electronic state

As in the previous case of methyl torsion, we will use the components of the total energy to analyze the barrier to aldehyde inversion. The components for the planar-antieclipsed and the pyramidal fully optimized geometries are shown in Table 2. The change in magnitude of these quantities between the pyramidal fully optimized and the planar-antieclipsed conformations is $\Delta V_{en} = -0.33936$ a.u. and $\Delta V_{ee} = -0.13950$ a.u., respectively. Thus, the terms leading to the barrier are the attractive electron–nuclei, V_{en} and the repulsive electron–electron, V_{ee} potential energies. Therefore, the barrier to inversion is mainly due to the increase of stability of the V_{en} term rather than to a decrease in repulsive interactions V_{ee}.

A simple picture can be drawn to interpret the pyramidalization phenomenon. In the S_0 state, the C_2 atom is sp^2 hybridized. In the S_1 state, however, it loses the π component of the double bond to the O_3 atom. Without the π structure to stabilize the sp^2 hybridization, the C_2 atom adopts an almost sp^3-like hybridization which produces the pyramidalization. This change in hybridization agrees with the decrease of the C_1–C_2–O_3 angle from 117.27° to 113.99° and of the H_4–C_2–C_1 angle from 127.41° to 119.40°. The change in the C_1–C_2 bond length from 1.488 to 1.498 Å also is in agreement with this point of view.

Conclusions

The experimental data for the S_1 state are somewhat sparse. Baba et al. [11] have fitted the wagging and torsional progression to uncoupled one-dimensional anharmonic oscillators. In their treatment they find a value of 687–691 cm^{-1} for the barrier to internal rotation and 541–670 cm^{-1} for molecular inversion. Our value of 677.9 cm^{-1} is in reasonable agreement with the torsional barrier but the inversion barrier at 1093.0 cm^{-1} is much higher. Our calculated inversion barrier however, does compare well with the calculated barrier of Crighton and Bell [8] who obtained a value of 1371 cm^{-1}. The discrepancy between the calculated and the observed values may be due to the coupling between the two anharmonic oscillators. However, from the magnitude of the differences a more likely source would be the lack of corrections for electron correlation. The effect of the correlation energy on the barrier to inversion is at present under study.

The potential energy surface $V(\theta, \alpha)$ for the S_0 state contains three minima which represent the positions of equilibrium stability in the molecule. In the direction of α wagging the potential has only a single minimum with steep sides as would be expected for a vibrational mode which is essentially harmonic and of small amplitude. In comparison, the S_1 excited state contains six minima, representing six possible positions of stability. In this case a maximum in the potential surface is obtained for $\theta = 0°$, $\alpha = 0°$ while for the S_0 ground state the potential is at minimum for these positions. Thus, in the upper state, acetaldehyde possesses a structure which is very different from the ground state in that it is distorted from the plane of the molecule, while at the same time, the methyl group is rotated with respect to the molecular frame. Coupling between the methyl torsion and wagging motions has the effect of rotating the axes through the elliptical isopotential lines around the minima. While this effect is clear in the S_0 state, the contour lines for the S_1 state are mainly circular at the bottom of the well.

It is found that the methyl torsion barriers in both electronic states can be considered to result from global effects rather than only involving the methyl group. It is possible to associate the preference of an eclipsed conformation in the S_0 state to an increase in the in-plane bonding interaction and to a decrease of the out-of-plane antibonding interaction between the methyl group and the O_3 atom. This hyperconjugation is unusual because it involves the oxygen atom which has in-plane and out-of-plane p orbitals that are able to interact with the methyl pseudoatom (in a similar way to the case of the barriers to rotation arising from σ and π bonding interactions between non bonded atoms in three heavy-atoms systems [29]). This fact would explain the differences between the in-plane and the out-of-plane methyl C–H stretching frequencies observed in carbonyl compounds.

The hyperconjugative model also explains the change in the conformational preference that occurs on excitation from the S_0 to the S_1 excited state. This change in conformation is a consequence of several factors, namely, a decrease in charge on the in-plane $2p_y$ orbital and an increase in the out-of-plane $2p_z$ orbital of the oxygen atom. Secondly, there is a change to antibonding character in the $2p_z$ excited state orbital.

The inversion barrier in the S_1 electronic state is found to arise principally from an attractive interaction instead of a pure repulsive one. The more stable pyramidal conformation results from the adoption of a pseudo-sp^3 hybridization by the C_2 carbonyl atom.

References

1. Clouthier DJ, Moule DC (1989) Periodic Group Relationships in the Spectroscopy of the Carbonyls, Ketenes and Nitriles: The Effect of Substitution by Sulfur, Selenium, and Phosphorus. In: Dewar MJS, Dunitz JD, Hafner K, Heilbronner E, Ito S, Lehn J-M, Niedenzu K, Raymond KN, Rees CW, Vögtle F (eds) Topics in Current Chemistry, vol 150, Springer, Berlin, pp 167–247
2. Noble M, Lee EKC (1984) J Chem Phys 81:1632
3. Del Bene JE, Worth GT, Marchese FT, Conrad ME (1975) Theor Chim Acta 36:195
4. Bernardi F, Robb MA, Tonachini G (1979) Chem Phys Lett 66:195
5. Wiberg KB, Walters V, Colson SD (1984) J Phys Chem 88:4723
6. Wiberg KB, Martin E (1985) J Am Chem Soc 107:5035
7. Ozkabak AG, Goodman L (1992) J Chem Phys 96:5958
8. Crighton JS, Bell S (1985) J Mol Spectrosc 112:285
9. Baba M, Nagashima U, Hanazaki I (1985) J Chem Phys 83:3514
10. Kilb RW, Lin CC, Wilson Jr EB (1957) J Chem Phys 26:1695
11. Baba M, Hanazaki I, Nagashima U (1985) J Chem Phys 82:3938
12. Fink WH, Allen LC (1967) J Chem Phys 46:2276
13. Jorgensen WL, Allen LC (1970) Chem Phys Lett 7:483; Jorgensen WL, Allen LC (1971) J Am Chem Soc 93:567
14. Liberles A, O'Leary B, Eilers JE, Whitman DR (1972) J Am Chem Soc 94:6894
15. Moule DC, Ng KHK (1985) Can J Chem 63:1378
16. Walsh AD (1953) J Chem Soc 2036
17. Dupuis M, Spangler D, Wendoloski JJ (1980) in: National Resource for Computations in Chemistry, Software Catalog. University of California. Berkeley, CA. Program QG01; Schmidt MW, Boatz JA, Baldridge KK, Koseki S, Gordon MS, Elbert ST, Lam B (1987) QCPE Bull 7:115; Schmidt MW, Baldridge KK, Boatz JA, Jensen JH, Koseki S, Gordon MS, Nguyen KA, Windus TL, Elbert ST (1990) QCPE Bull 10:52
18. Hariharan PC, Pople JA (1973) Theor Chim Acta 28:213
19. Smeyers YG, Niño A, Bellido MN (1988) Theor Chim Acta 74:259
20. Broyden CG (1970) J Inst Maths Appl 6:76; Fletcher R (1970) Comp J 13:317; Goldfard D (1970) Math Comp 24:23; Shanno DF (1970) Math Comp 24:647
21. Nösberger P, Bauder A, Günthard HH (1973) Chem Phys 1:418; Harmony MD, Laurie VW, Kuczkowski RL, Schwendeman RH, Ramsay DA, Lobas FJ, Lafferty WJ, Maki AG (1979) J Phys Chem Ref Data 8:619
22. McKean DC (1978) Chem Soc Rev 7:399
23. Pople JA, Gordon M (1967) J Am Chem Soc 89:4253
24. Kleiner I, Hougen JT, Suenram RD, Lovas FJ, Godefroid M (1991) J Mol Spectrosc 148:38; Kleiner I, Hougen JT, Suenram RD, Lovas FJ, Godefroid M (1992) J Mol Spectrosc 153:578
25. Allen LC (1968) Chem Phys Lett 2:597
26. Neumann D, Moskowitz JW (1968) J Chem Phys 49:2056
27. Hellmann H (1937) in: Einführung in der Quantemchemie, Deuticke, Leipzig, p 285; Feynman RP (1939) Phys Rev 56:340
28. Mulliken RS, Rieke CA, Brown WG (1941) J Am Chem Soc 63:41
29. Dill JD, Schleyer PR, Pople JA (1976) J Am Chem Soc 98:1663